DIFFUSION OF INERTIAL PARTICLES IN A TURBULENT GAS JET

T. A. Girshovich and V. A. Leonov

UDC 532.517.4

An algorithm is proposed and a mathematical experiment is performed on the diffusion of high-density particles in a turbulent gas jet. The problem is solved with the impurity particle action on the carrier phase characteristics taken into account.

As is known, high-density particle diffusion in a turbulent jet differs in principle from gas impurity diffusion [1, 2], as is expressed by the fact that the impurity particle concentration profiles in the jet are significantly narrower than the carrier phase velocity profiles while the gas impurity concentration profile is broader than the velocity profile.

Investigation of inertial particle diffusion in a turbulent jet flow field is of considerable scientific and practical interest and since it is quite difficult to realize a direct physical experiment on particle diffusion at this time, execution of a mathematical experiment merits attention. Such an experiment is performed in [3-5] under assumptions about the passive role of the impurity in the jet and Stokes particle flow, which is valid for very small initial impurity concentrations and low Reynolds numbers of the particle flow.

The formulation and results of a mathematical experiment performed within the framework of the Prandtl turbulence model according to a scheme analogous to [3] but with changes in the carrier phase characteristics under the action of the impurites taken into account, are considered below. Moreover, the particle drag in this experiment was determined by the general formula [6] that is valid in a broad range of Reynolds number variation.

The solution of the problem is sought in a Lagrange formulation with subsequent statistical estimates of totals of a large number of realizations, i.e., transists of the very same particle from its location at the nozzle exit to a given section. It is considered that the particle moves under the effect of turbulent moles and a large number of random successive particle displacements is realized together with such moles during each realization. Motion occurs in one mole either during its "lifetime" or the time of mole intersection by a particle if the difference in their velocities is large. A new mole with its own characteristics captures the particle during this time. The particle with the new mole are incident at a new point and so on until the section in which we are interested is reached.

The motion trajectory is evolved during the successive integration of the particle motion equation over the extent of its displacement with each gas mole.

The particle equation of motion has the form

$$m\frac{dV_p}{dt}=C_x\frac{\rho_g(V_g-V_p)|V_g-V_p|}{2}F_p. \qquad (1)$$

The particle drag coefficient in the gas steam C_x was determined from the formula [6]

$$C_x=0.32+\frac{4{,}3}{\sqrt{\mathrm{Re}}}+\frac{24}{\mathrm{Re}}, \qquad (2)$$

where $\mathrm{Re}=\rho_g|\boldsymbol{V}_g-V_p|d_p/\mu_g$.

Making the natural assumption for jet flow that the transverse velocity in the jet is much less than the longitudinal velocity, and making the velocity dimensionless by means of the initial gas velocity, and the time by means of (r_0/μ_{g_0}), we obtain the following particle motion equations

Sergo Ordzhonikidze Moscow Aviation Institute. Translated from Inzhenerno-Fizicheskii Zhurnal, Vol. 57, No. 3, pp. 367-375, September, 1989. Original article submitted April 19, 1988.

$$\psi(u_p)\frac{du_p}{dt}=u_g-u_p, \tag{3}$$

$$\psi(u_p)\frac{dv_p}{dt}=v_g-v_p. \tag{4}$$

Here

$$\psi(u_p)=\frac{\mathrm{Stk}}{1+0{,}0133\,\psi_1+0.179\,\psi_1^{1/2}}, \tag{5}$$

where Stk is the Stokes number

$$\mathrm{Stk}=\frac{\rho_s u_{g0} d_p^2}{18\,\mu_g r_0}, \tag{6}$$

$$\psi_1=\mathrm{Re}_0\,|u_g-u_p|=\frac{\rho_g u_{g0} d_p}{\mu_g}\,|u_g-u_p|. \tag{7}$$

The instantaneous gas velocities are determined as the sum of the average and the fluctuating components

$$u_g=\bar{u}_g+u_g',\quad v_g=\bar{v}_g+v_g'. \tag{8}$$

Considering the profiles of the relative average longitudinal gas velocities similar in the jet, we use the Schlichting formula for their description. The transverse average gas velocity components are found from solutions of the appropriate continuity equations. In the jet core we have for the average velocity components according to the gas velocity

$$\frac{u_g}{u_{g0}}=1,\quad \frac{v_g}{u_{g0}}=0. \tag{9}$$

The fluctuating gas velocities u_g' and v_g' are determined as random variables normally distributed with zero mathematizal expectation and variance equal to the r.m.s. value of the fluctuating velocity $\sqrt{u_g^{\prime 2}}$, determined with influence of the inertial impurity on the turbulent structure taken into account according to the G. N. Abramovich–T. A. Girshovich model [7]

$$\sigma=\sqrt{u_{g0}^{\prime 2}}\,\frac{1+\varkappa u_{\sim}'/u_{g0}'}{1+\varkappa}. \tag{10}$$

The r.m.s. fluctuation velocity of a pure gas is here determined in conformity with the Prandtl turbulence theory from the formula

$$\sqrt{u_{g0}^{\prime 2}}=l_u\left|\frac{\partial u}{\partial y}\right|, \tag{11}$$

where ℓ_u is the mixing path that is considered constant and proportional to its width in the given jet section, $u_{\sim}'$ is the relative gas velocity fluctuation $u_{\sim}'=u_g'-u_p'$ determined by the formula

$$\ln\frac{|u_{\sim}'|}{|u_{\sim 0}'|}=-\frac{2\,l_u N(1+\varkappa)^2}{|u_{g0}'+(1+2\varkappa)\,u_{p0}'-u_{\sim}'|}, \tag{12}$$

where $N = 18\,\mu_g/\rho_s d_p$; and u_{p0}' is the particle initial velocity in the mole whose magnitude lies in an interval between zero and u_{g0}' depending on the relaxation time [8].

The average characteristics of a two-phase jet must be determined many times during one realization and in a large number of realizations when performing a mathematical experiment. To reduce the volume of calculational work, the jet characteristics computed earlier for the initial, transition, and main sections were approximated for each specific case by two parameters, the distance from the nozzle exit and the initial impurity concentration.

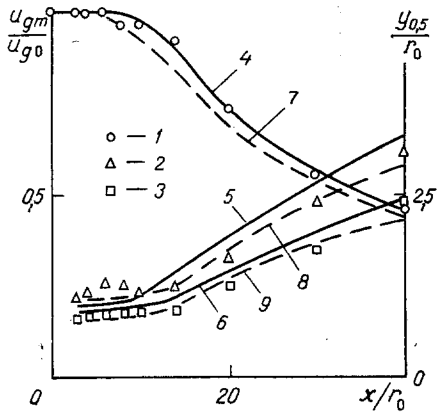

Fig. 1

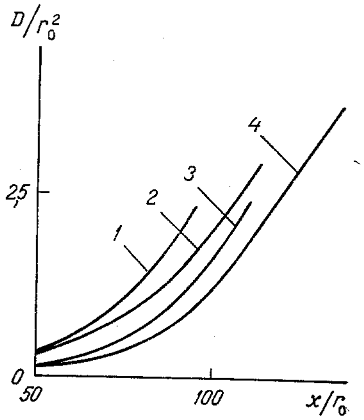

Fig. 2

Fig. 1. Axial velocity and boundary of a jet with bronze particles of 8500 g/m^3 density, 45 μm diameter for an initial 1.0 kg/kg impurity concentration. Experiment: 1) gas axial velocity; 2) jet boundary at half the gas velocity; 3) jet boundary at half the impurity concentration. Computation: 4, 5, 6) axial gas velocities; jet boundary at half the gas velocity and half the concentration calculated by the proposed integral method; 7, 8, 9) the same by the method of [12].

Fig. 2. Variance of the particle transverse displacement: 1, 3) initial impurity concentration $\varkappa_0 = 0$; 2, 4) $\varkappa_0 = 1,0$; 1, 2) obtained when using the general law for particle drag in a gas stream; 3, 4) for Stokes particle flow.

The jet characteristics were determined by using the integral method developed for the initial and main sections of two-phase jets [7, 9, 10] and supplemented by a computation of the jet transition section. The axial parameters in the transition section between the initial and main sections in pure gas jets can be considered constant with a certain approximation and equal to their initial values [11]. However, it must be noted that the transition section in pure gas jets is comparatively short and the drop of the axial parameters, as compared with the initial, is barely noticeable therein. As the initial impurity concentration grows in two-phase jets, the jetlong range, and therefore, the transition section length grows and can be quite large, and consequently, the drop of the axial parameters with distance from the jet exit should be noticeable.

Since conversion of the velocity and concentration profiles from the initial section profiles to main section profiles occurs in the transition section, then it is logical to give formulas for the velocity and concentration in the transition section in the form of superposition of these profiles

$$\frac{u_g}{u_{gm}} = [1 - \gamma(x)]\, f_{1u}(\eta_u) + \gamma(x)\, f_{2u}(\eta_u), \tag{13}$$

$$\frac{\varkappa}{\varkappa_m} = [1 - \beta(x)]\, f_{1\varkappa}(\eta_\varkappa) + \beta(x)\, f_{2\varkappa}(\eta_\varkappa). \tag{14}$$

Here f_{1u}, $f_{1\varkappa}$ are the Schlichting expressions for the gas velocity and impurity concentration profiles in the initial section

$$f_{1u} = 2(1-\eta_u)^{3/2} - (1-\eta_u)^3, \;\; f_{1\varkappa} = 2(1-\eta_\varkappa)^{3/2} - (1-\eta_\varkappa)^3, \tag{15}$$

and f_{2u}, $f_{2\varkappa}$ in the main section

$$f_{2u} = (1-\eta_u^{3/2})^2, \;\; f_{2\varkappa} = (1-\eta_\varkappa^{3/2})^2, \tag{16}$$

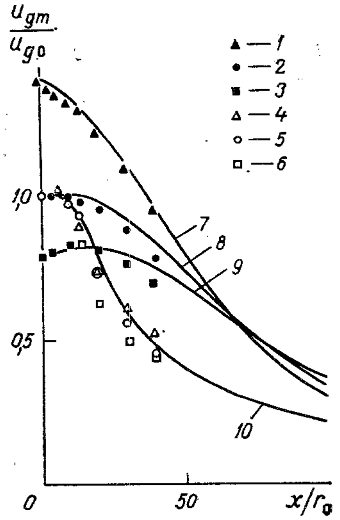

Fig. 3

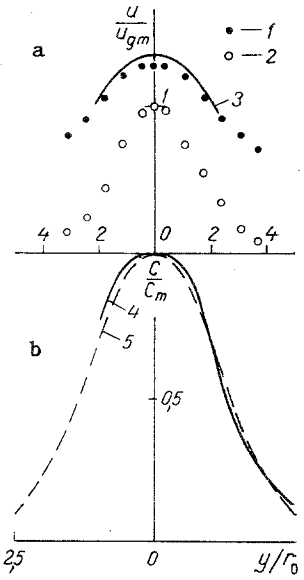

Fig. 4

Fig. 3. Axial particle and gas velocities for different values of the initial dynamic nonequilibrium: 1-3, 7-9) particle velocity; 4-6, 10) gas velocity; 1, 4, 7) u_{p0} = 35 m/sec; u_{g0} = 25 m/sec; 2, 5, 8) u_{p0} = 35 m/sec; 3, 6, 9) u_{p0} = 35 m/sec; u_{g0} = 45 m/sec; 10) gas velocity calculated by using the integral method for dynamically equilibrium efflux of a two-phase mixture.

Fig. 4. Comparison of computed and experimental data by profiles of the average longitudinal velocity and concentration of the particles. Experiment: 1) particle velocity; 2) gas velocity; 4) particle mass concentration. Computation: 3) particle velocity; 5) particle mass concentration.

$\gamma(x)$, $\beta(x)$ are the deformation functions that were given in the form of third-degree polynomials whose coefficients were determined from the conditions of a smooth transition of the initial section velocity and concentration profiles into the corresponding main section profiles. These formulas have the form

$$\gamma(x) = 3\left(\frac{x - x_i}{x_{tu} - x_i}\right)^2 - 2\left(\frac{x - x_i}{x_{tu} - x_i}\right)^3, \tag{17}$$

$$\beta(x) = 3\left(\frac{x - x_i}{x_{tu} - x_i}\right)^2 - 2\left(\frac{x - x_i}{x_{\text{пк}} - x_i}\right)^3. \tag{18}$$

The abscisses of the transition section ends in the gas velocity and the impurity concentration were determined by a linear continuation of the initial section boundary to the initial sections of the main sections in the velocity and concentration [11].

The computed axial velocities and the jet boundaries are compared to test data [2] and results of numerical integration of the motion and continuity equations [12] are compared in Fig. 1. It is seen that the computation by the proposed integral method that takes account of the change in the axial parameters in the transition section permits a satisfactory description of the average two-phase jet characteristics. It must be noted that the computation method described above was developed under the assumption of equality of the average particle and gas velocities. However, as will be shown below, the tests indicate that nonequilibrium of the flow has slight influence on the gas phase characteristics.

In conformity with the Prandtl theory, it is considered that the gas velocity fluctuation components u_g' and v_g' are equal and that the instantaneous mean velocity of a gas mole is conserved during its "lifetime". The particle motion equations (3) and (4) can be integrated numerically under the following initial conditions

$$u_p = u_{pi}, \quad v_p = v_{pi} \quad \text{for} \quad t = t_i. \tag{19}$$

Here u_{pi} and v_{pi} are the particle velocities incident in the (k + 1)-th mole at the beginning of its "lifetime".

As was noted above, the time of particle interaction with a turbulent mole is determined as the minimal of the "lifetime" of a given mole and the time of particle residency in the mole if the difference between the mole and particle velocities is large:

$$T = \frac{l_u}{(\sqrt{u_g'^2 + 2v_g'^2})_{\max}} \quad \text{or} \quad T = \frac{l_u}{|u_g - u_p|}. \tag{20}$$

The computation is performed in the following order. The initial particle coordinates and velocities, the initial gas velocity, and the initial impurity concentration are given at the nozzle exit. A certain time after the start the particle moves in the core of a constant gas velocity, then it drops into the mixing zone where the first turbulent mole is entrained, it moves with it for a time T and is incident at the point (x_p, y_p) having the velocity u_p and v_p. It is assumed that a new mole is formed at this point, in which the particle will move during the following time interval and so on. Passing the initial section the particle is incident in the transition and then in the main section constantly performing disordered random motion.

The particle velocity components and its coordinates are determined at each of the N realizations at given fixed times t_k. Then the mean quantities $\langle x_p\rangle$, $\langle y_p\rangle$, $\langle y_p^2\rangle$,$\langle u_p\rangle$, $\langle u_p^2\rangle$, $\langle v_p\rangle$, $\langle v_p^2\rangle$. over the number of particles (the number of realizations) are determined at these same times. The variance of the particle transverse displacement

$$D(t_k) = \frac{\sum_{i=1}^{N} y_p^2}{N} - \frac{\left(\sum_{i=1}^{N} y_p\right)^2}{N} \tag{21}$$

and the particle diffusion coefficient

$$D_p = 0{,}5\,\frac{d}{dt}[D(t_k)]. \tag{22}$$

can afterwards be determined.

The r.m.s. deviation of the quantities u_p and v_p, i.e., u_p' and v_p', can be calculated analogously to (21).

For confidence in the estimates the number N should be sufficiently large. The preliminary computations show that the number N must be chosen within limits from 200 and higher depending on up to what distance from the nozzle exit the characteristics are estimated.

The time t_k is a parameter that can be eliminated and the following dependence can be obtained

$$y_p = f(x_p),\ u_p = f(x_p,\ y_p),\ v_p = f(x_p,\ y_p),\ D_p = f(x_p,\ y_p). \tag{23}$$

The influence of the initial impurity concentration on the change in the variance of the transverse particle displacement with distance from the nozzle is shown in Fig. 2. Computations are performed for the particles utilized in tests [3] with a 2000 kg/m^3 density and 20 μm size. The graphs clearly show that the impurity concentration exerts a noticeable influence on the variance of the transverse particle displacement, which confirms the necessity for taking account of the action of the inertial impurity on the jet characteristics in the numerical experiment. The graphs also show the significant difference in the determination of the variance when calculating the particle drag coefficient by the general formula and by the Stokes formula utilized in computations [3-5].

Presented in Fig. 3 is a comparison of the computed values of the axial velocities of bronze particles of 8500 kg/m^3 density and 45 μm diameter for an initial impurity concentration 1.0 with the experimental data described in [2] for different values of the initial dynamic nonequilibrium. The points here correspond to the experimental data and the lines to the computed results.

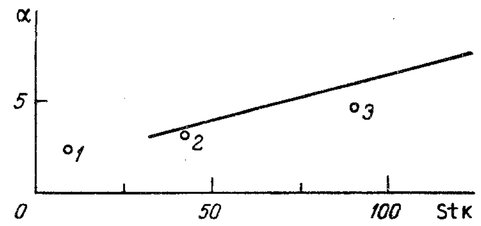

Fig. 5. Dependence of the analog of the Schmidt number on the Stokes number: 1) u_{g0} = 49 m/sec; d_p = 16.5 μm; $\varkappa_m$ = 0.1; 2) u_{g0} = 52 m/sec; d_p = 34 μm; $\varkappa_m$ = 0.05; 3) u_{g0} = 54.5 m/sec; d_p = 48.7 μm; $\varkappa_m$ = 0.34.

Having been given different initial particle locations on the nozzle exit; the distributions of the appropriate particle velocities, concentration, diffusion coefficient and Schmidt number can be obtained at given jet sections.

The particle concentration profiles can here be determined by statistical estimates of the particle distribution density in the jet sections under consideration. The estimates are performed for Nn realizations, where N is the number of particles escaping from the fixed point and n is the number of points on the nozzle exit from which the particles escaped. The radius of the given jet transverse section is divided into m intervals. Then the frequencies n_i of particle incidence in each of the m elementary rings are determined. The variance

$$D = \sigma^2 = \sum_{i=1}^{m} y_i^2 P_i \tag{24}$$

is calculated from this data by means of the formula in [13]. Here y_i is the mean radius of the ring element, and $P_i = n_i/Nn$ is the frequency of particle incidence in the -th ring.

Taking account of the bell-shaped form of the concentration profile, it can be considered that the particle concentration distribution in the jet transverse section is described by a Gauss curve with the mathematical expectation zero and the variance σ_p^2 found from a mathematical experiment by means of (24)

$$\frac{C}{C_0} = \frac{C_m}{C_0} \exp\left(-\frac{r^2}{2\sigma_p^2}\right). \tag{25}$$

Taking into account that the relative magnitude of the particle longitudinal velocity can be approximated by a Gauss curve

$$\frac{u_p}{u_{pm}} = \exp\left(-\frac{r^2}{2\sigma_u^2}\right), \tag{26}$$

we obtain the expression

$$\frac{C_m}{C_0} = \frac{1}{2}\left(\frac{1}{\sigma_p^2} + \frac{1}{\sigma_u^2}\right)\frac{u_{p0}}{u_{pm}}, \tag{27}$$

from the conditions of conservation of the impurity flow rate in the jet transverse section for the axial mass concentration, from which we find for the relative discharge concentration

$$\frac{\varkappa_m}{\varkappa_0} = \frac{C_m}{C_0}\frac{u_{pm}}{u_{p0}} = \frac{1}{2}\left(\frac{1}{\sigma_p^2} + \frac{1}{\sigma_u^2}\right). \tag{28}$$

It has been found that the computed profile of the relative longitudinal velocity of glass balls with 2990 kg/m³ density and 50 μm diameter are in completely satisfactory agreement with the experimental data presented in [14] for an 0.32 initial concentration in the section x/r_0 = 40. However, an estimation of the velocity and concentration profiles for bronze particles [2] according to the scheme proposed above showed that the profiles are narrower than the experimental. This discrepancy can be a result of the fact that not all the factors acting in the physical experiment were taken into account in the numerical investigations, for example, the particle rotation, or other effects inherent to the given tests.

Taking account of particle rotation with an angular velocity equal to the local vorticity of the stream showed that particle dissipation increased hardly noticeably under this assumption.

Taking account of the structural features of the apparatus shaping the mixture flow from the tube [15] in which the flow mode was given by using two-phase mixture suction from peripheral jet domains, we inserted the initial particle transverse velocity into the computation. From symmetry considerations it can here be considered that the transverse velocity depends on the distance to the axis and, as in [6], the expression for the transverse velocity would be taken in the form

$$\frac{v_{g0}}{u_{g0}} = K\frac{r}{r_0}. \tag{29}$$

Computed and test profiles of the average longitudinal velocity and concentration of bronze particles [2] of 45 μm diameter are compared in Fig. 4 in the $x/r_0 = 20$ jet section for an initial impurity concentration 1.0 and a value 0.05 for K in (29). The comparisons were performed for the equilibrium case of two-phase jet efflux at an initial 35 m/sec velocity. The graphs indicate satisfactory agreement between the computed and test data.

The change in the computed value of the analog of the Schmidt number

$$\alpha = \frac{l_u}{l_\varkappa} = \frac{\nu_T}{D_p}\frac{\sqrt{\overline{v_p'^2}}}{\sqrt{\overline{v_g'^2}}} \tag{30}$$

as the Stokes number grows is shown in Fig. 5.

The computation was performed in the section $x/r_0 = 50$ for $\eta_u = 0.22$ and $\varkappa_0 = 0$. It is seen that as the Stokes number grows, i.e., as the particle inertia grows, the analog of the Schmidt number grows as should have been expected. The quantity α determined by the method of [8, 9] for the corundum particles used in the tests [1] is shown by points in this same graph.

The graph shows that the method proposed in [8, 9] permits a quite satisfactory estimation of the magnitude of the analog of the Schmidt number that must be known to obtain the impurity distribution in the jet transverse sections.

The comparison shown above between the results of the mathematical and physical experiments indicates that the algorithm described and the corresponding program of the mathematical experiment permit computation of the average and fluctuating particle velocities, the particle concentration profile in a two-phase jet, the diffusion coefficient, the tangential stresses (within the framework of the Prandtl theory of turbulence). These data together with the method described above for computing the average two-phase jet characteristics can be utilized in organizing the working processes of many technical units with a two-phase working body (thermal engines, chemical reactors, furnaces, etc.).

NOTATION

x, y, coordinate axes; x, along the jet axis; y, perpendicular to x; V, total instantaneous velocity; u,v, longitudinal and transverse velocity components, m, mass, t, time, ρ, density, F, area of the middle, d, diameter, r, radius; $\varkappa_0$, impurity discharge concentration; c, impurity mass concentration; μ, ν, dynamic and kinematic viscosities; η, dimensionless coordinate; $\eta = y/\delta$, δ jet half-width. Subscripts: 0, initial value; g, gas; p, particle; m, value on the jet axis; П, jet initial section; t, jet transition section; T, turbulent; and s, impurity substance.

LITERATURE CITED

1. M. K. Laats and F. A. Frishman, Izv. Akad. Nauk SSSR, Mekh. Zhidk. Gaza, No. 2, 186-191, (1970).
2. T. A. Girshovich, A. I. Kartushinskii, M. K. Laats, et al., Izv. Akad. Nauk SSSR, Mekhan. Zhidk. Gaza, No. 5, 26-31 (1981).

3. S. Yuu, N. Jasukouchi, U. Hirosava, and T. Jotaki, AIChE J., 24, No. 3, 509-519 (1978).
4. J.-S. Shuen, L.-D. Chen, and G. M. Faeth, AIChE J., 29, No. 1, 167-170 (1983).
5. A. Ormancey and J. Martinon, Physicochem. Hydrodyn., 5, No. 3-4, 229-244 (1984).
6. M. V. Kravtsov, Inzh.-Fiz. Zh., 15, No. 3, 464-470 (1968).
7. G. N. Abramovich and T. A. Girshovich, Vapor-liquid Flows [in Russian], Minsk (1977), p. 155-175.
8. G. N. Abramovich and T. A. Girshovich, Dokl. Akad. Nauk SSSR, 212, No. 3, 573-576 (1973).
9. G. N. Abramovich, V. N. Bazhanov, and T. A. Girshovich, Izv. Akad. Nauk SSSR, Mekh. Zhidk. Gaza, No. 6, 41-49 (1972).
10. G. N. Abramovich, ed., Theory of Turbulent Jets, 2nd rev. ed. [in Russian], Moscow (1984).
11. G. N. Abramovich, Theory of Turbulent Jets [in Russian], Moscow (1960).
12. L. B. Gavin, V. A. Naumov, and V. V. Shor, Prikl. Mekh. Tekh. Fiz., No. 1 62-67 (1984).
13. E. S. Ventsel', Theory of Probability [in Russian], Moscow (1962).
14. D. Modarres, H. Tan, and S. Elhobashi, Aerospace Engineering [Russian translation], 2, No. 12, 83-91 (1984).
15. M. K. Laats and F. A. Frishman, Turbulent Two-Phase Flows [in Russian], Tallinn (1979), pp. 158-165.
16. Yu. V. Zuev, M. K. Laats, and I. A. Lepeshinskii, Izv. Akad. Nauk SSSR, Mekh. Zhidk. Gaza, No. 4, 183-185 (1985),

UTILIZATION OF MODEL PASSIVE IMPURITY CONCENTRATION DISTRIBUTION FUNCTIONS TO COMPUTE TURBULENT FLOW RADIATION

Yu. V. Khodyko, A. I. Bril', and O. B. Zhdanovich UDC 536.3:532.517.4

The adequacy of different semi-empirical methods of taking account of passive impurity concentration fluctuations is investigated for numerical modelling of radiating turbulent flows on the basis of comparisons between computed and measured energetic brightness fields.

The rise in the accuracy of computations of energetic brightness fields of turbulent heated gas flows is associated with the solution of the problem of the influence of temperature and concentration fluctuations on the optical characteristics of a medium. The contribution of turbulent fluctuations to IR radiation of a heated gas jet was investigated in [1]. Since the range of temperature variation in the jet was not large (approximately 300-700 K), the fluctuation characteristics of the temperature field were considered similar to the fluctuation characteristics of the passive impurity concentration field. An analogous approach is used in the present research also. It was shown in [1] that satisfactory agreement between the experimental and computed data is achieved when using probability density functions (PDF) in which the appearance of intermittency in the jet is taken into account in a model fashion. In recent years, intermittency in jet type flows has been investigated quite intensively both theoretically and experimentally [2]. A number of PDF models has been proposed for passive impurity concentration with the intermittency taken into account [2-5]. The purpose of this paper is to confirm the possibility of utilizing such PDF to compute the radiation. Moreover, the influence of temperature and concentration fluctuations on the radiation is studied as a function of the initial turbulence level in the stream.

The measurements and computations were preformed for an axisymmetric subsonic heated jet. A description of the experimental installation and the method of measuring the gas dynamic parameters and the spectrum characteristics are presented in [1, 6].

The jet efflux conditions were changed by using different reducers for an unchanged mode of combustion chamber operation. Three modes were realized: mode 1 without the reducer (jet initial section radius R_0 = 15 cm, initial efflux velocity u_0 = 13 m/sec), mode 2 with two

Physics Institute, Belorussian Academy of Sciences, Minsk. Translated from Inzhenerno-Fizicheskii Zhurnal, Vol. 57, No. 3, pp. 375-382, September, 1989. Original article submitted April 20, 1988.